Ionics (2018) 24:2489–2498
https://doi.org/10.1007/s11581-017-2358-5

ORIGINAL PAPER

Voltammetric sensing of nitrite in aqueous solution using titanium dioxide anchored multiwalled carbon nanotubes

Mambo Moyo[1] · Prince Mudarikwa[1] · Munyaradzi Shumba[1] · Jonathan O. Okonkwo[2]

Received: 9 August 2017 / Revised: 31 October 2017 / Accepted: 14 November 2017 / Published online: 24 November 2017

Abstract

A glassy carbon electrode modified with TiO_2 anchored on multiwalled carbon nanotube particles was used for voltammetric determination of nitrite in phosphate buffer solution (pH 7). Characterization of modified electrodes was performed using transmission electron microscopy (TEM), energy dispersive X-ray spectrometer (EDS), and voltammetric techniques. Under optimal conditions, TiO_2/MWCNT/GCE reduced oxidation potential by 250 mV and enhanced i_{pa} by 2.7-fold (≈ 172%) higher when compared with bare glassy carbon electrode. A linear voltammetric response from 0.02 to 600 μM with a detection limit of 0.011 μM ($s/n = 3$) was obtained using DPV. The apparent diffusion coefficient for nitrite was calculated to be 2.15×10^{-6} cm^2 s^{-1}. The fabricated sensor was used for the determination of nitrite in water samples and the results were consistent with the values obtained by the ultraviolet–visible spectroscopy (UV-Vis) method.

Keywords Nitrite · Nano TiO_2 · Multiwalled carbon nanotube · Voltammetry

Introduction

Nitrite is an inorganic anion composed of a nitrogen atom bonded to two oxygen atoms. Its use as a preservative in food industry and as a corrosion inhibitor during industrial water preparation has been highlighted [1–5]. The effect of high concentrations of nitrite in environmental water bodies and human health has been discussed [3, 6, 7]. The maximum limit of nitrite in water samples should not exceed 3 mg L^{-1}, according to World Health Organization [8]. Hence, it is necessary to develop a simple and selective sensor for continuous monitoring of nitrite so that if recommended limits by regulatory bodies are exceeded then remediation techniques can be sought quickly without posing environmental harm.

Literature survey reveals that different instrumental techniques have been used for nitrite determination with great success [9–13]. However, time-consuming, high costs of the equipments, and the need for qualified technicians have been cited as some drawbacks [14]. In an attempt to rectify this, electrochemists have shifted to voltammetric techniques as an option as evidenced by working principles which are easy to follow when monitoring environmental samples [15, 16]. Furthermore, voltammetric techniques involving exploitation of chemically modified electrodes (CMEs) incorporating different modifiers [2, 3, 5, 15–22] have been reported for electro-oxidation of nitrite.

The use of carbon nanotubes in electrochemical sensing of numerous environmental pollutants has received attention [14, 15, 23] mainly due to their small particle size, enhanced voltammetric peaks, and high electronic conductivity [24, 25]. On the other hand, metal and metal oxide nanoparticles are the mostly widely employed nanomaterials due to excellent and catalytic properties. TiO_2 has been used in sensor fabrication [20, 26–29] due to low cost, non-toxicity, large surface area, strong adsorptive ability, high uniformity and excellent catalytic activity [29]. In continuation of our studies involving CMEs [14], carbon nanotubes were used as substrates for anchoring TiO_2 nanoparticles in order to provide influence on morphology and electrochemical responses of nitrite through oxidation process since there is no interference from nitrate and molecular oxygen [15, 16, 30]. The ease of fabrication, simplicity, and low-detection limit are the main advantages of this sensor over the previous reported ones.

✉ Mambo Moyo
moyom@staff.msu.ac.zw

[1] Sensor Laboratory Research Group, Department of Chemical Technology, Midlands State University, Private Bag 9055, Senga, Gweru, Zimbabwe

[2] Department of Environmental, Water, and Earth Sciences, Tshwane University of Technology, 175 Nelson Mandela Drive, Arcadia Campus, Pretoria 0001, South Africa

Experimental

Materials

Phosphate buffer solutions (as supporting electrolyte) with different pH values were prepared by mixing standard stock solutions of 0.10 M Na_2HPO_4 and 0.10 M NaH_2PO_4. $NaNO_3$, $K_3Fe(CN)_6$, $K_4Fe(CN)_6$, *N*,*N*-dimethylformamide (DMF), TiO_2 nanopowder and MWCNT were obtained from Sigma-Aldrich (South Africa). All solutions were prepared using ultra Millipore water from Milli-Q Water Systems (Millipore Corp. Bedford, MA, USA). The purification of MWCNTs to remove metal oxide catalysts was followed as reported [2].

Equipment

Transmission electron microscopy (TEM) image was obtained from a Zeiss Libra TEM 120 model operated at 90 kV using carbon-coated 200 mesh grids. The energy dispersive X-ray spectrometer (EDS) images were obtained using a TESCAN Vega TS 5136LM electron microscope. Cyclic voltammetry (CV), electrochemical impedance spectroscopy (EIS), chronoamperometry, linear sweep voltammogram (LSV), and differential pulse voltammetry (DPV) were performed using an Autolab potentiostat PGSTAT 302F (Eco Chemie, Utrecht, Netherlands) equipped with NOVA 1.10 software.

Preparation of TiO_2/MWCNT nanocomposite

An appropriate ratio of MWCNT:TiO_2 (3:1 *w*/*w*) was mixed and then suspended in 80 mL of Millipore water through sonication for 30 min. The suspension obtained after sonication was magnetically stirred for 12 h and the precipitate obtained thoroughly washed with Millipore water using centrifugation process for 30 min and then dried prior to electrode modification.

Modification of electrodes

A three-electrode system was used with glassy carbon electrode (GCE) as working electrode, an Ag/AgCl (saturated KCl) reference electrode and platinum wire auxiliary electrode. The GCE was polished to a mirror finish with alumina slurry (0.3 μm). The electrode was sonicated in Millipore water for 5 min during the three successive cleaning stages and finally dried in a stream of nitrogen. The drop dry technique was employed for electrode modification. TiO_2, MWCNT, and TiO_2/MWCNT composite (1 mg mL^{-1}) in DMF were used as electrode modifiers to give TiO_2/GCE, MWCNT/GCE, and TiO_2/MWCNT/GCE which were stored at room temperature when not in use.

Results and discussion

Microscopic characterization

A monodispersion of TiO_2 nanoparticles with almost homogeneous size is confirmed by TEM image (Fig. 1). Black dots represent nanoparticles of average size 19 nm that are present on the image as depicted on the corresponding histogram (*inset*) showing size distribution. These characteristic features are good in electrochemical sensing.

EDS was further used to show the elemental composition of MWCNT (Fig. 2a) and TiO_2/MWCNT composite (Fig. 2b). Carbon was mainly observed upon modification with MWCNT alone. However, titanium and oxygen emerged after introduction of the nanosized TiO_2. The aluminum signal evident in the EDS spectrum could be coming from the aluminum sample holder used during analysis.

CV and EIS studies on modified GCE

Cyclic voltammetry (Fig. 3a) and electrochemical impedance spectroscopy (Fig. 3b) were employed to study the electron transfer ability of the modification process in 1 mM $[Fe(CN)_6]^{3-/4-}$ containing 0.1 M KCl. Table 1 shows the difference between anodic and cathodic peak potential (ΔE_p) of the modified electrodes. It has been highlighted that a low value of ΔE_p reflects good electron transfer for the redox probe [23]. The trend in electron transfer in the redox probe is: TiO_2/GCE (102 mV) < bare GCE (92 mV) < MWCNT/GCE (85 mV) < TiO_2/MWCNT/GCE (80 mV). The results confirmed that anchoring TiO_2 on MWCNT offered fast electron transfer ability.

In the EIS technique, the semicircle part at higher frequencies represents the electron transfer limited process and its diameter is equated to the electron transfer resistance (R_{ct}). From the Nyquist plots (Fig. 3b) and Table 1, the GCE (295 Ω) displays a small semi-circle indicating a low transfer resistance. The TiO_2/GCE (390 Ω) has a larger diameter suggesting that TiO_2 acted as insulating layer and barrier. The MWCNT/GCE (190 Ω) showed less resistance. An almost straight line and a small circle portion which was quite small was observed on the TiO_2/MWCNT/GCE and might be due to increase in reactive area, reduced interfacial resistance, and the composite making the electron transfer faster. Such small R_{ct} values characterized by relatively small differences between them for different probes have been reported before for probes designed for different analytes [31, 32]. The obtained results are in good agreement with peak current (i_{pa}) values obtained from CV measurements (Fig. 3c). The information from the Bode plots (Fig. 3d) further supports that modified surfaces have different behaviors since their phase angles shifted to different frequencies.

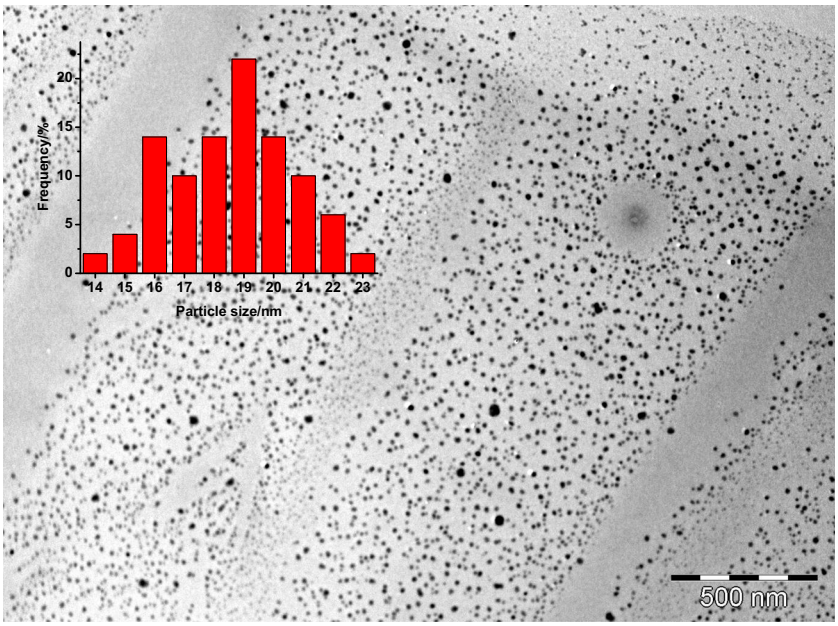

Fig. 1 TEM image for TiO_2 modifier. Corresponding histogram (*inset*)

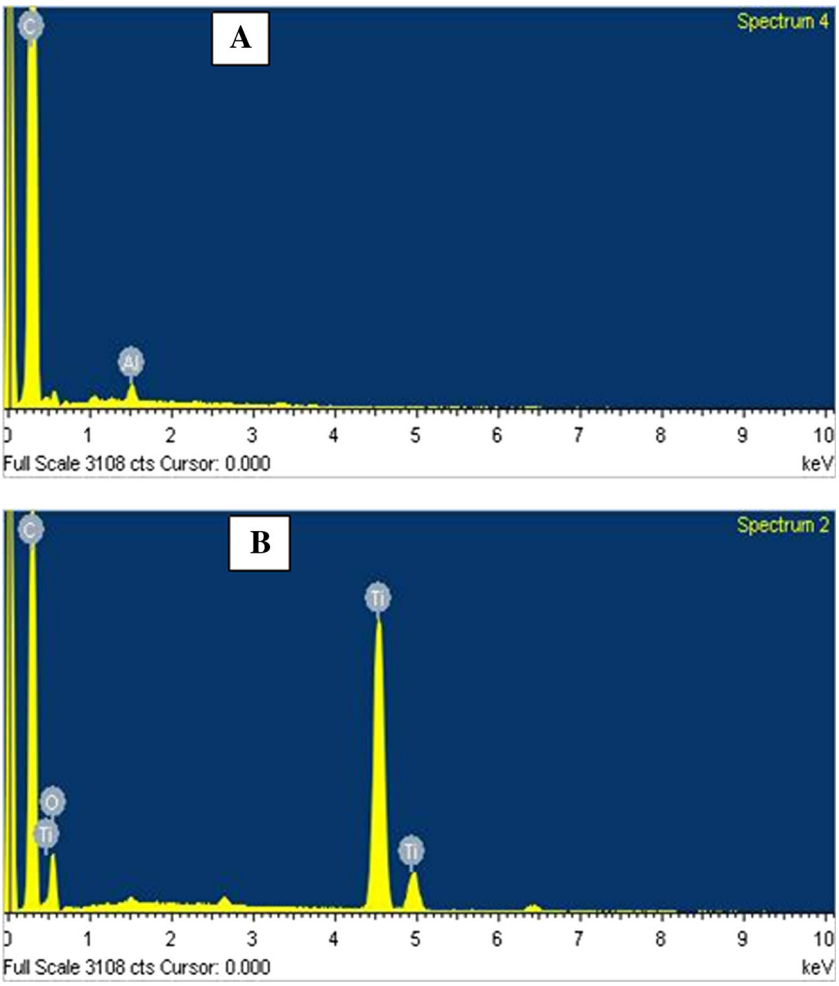

Fig. 2 EDS for (**a**) MWCNT (**b**) TiO_2/MWCNT composite

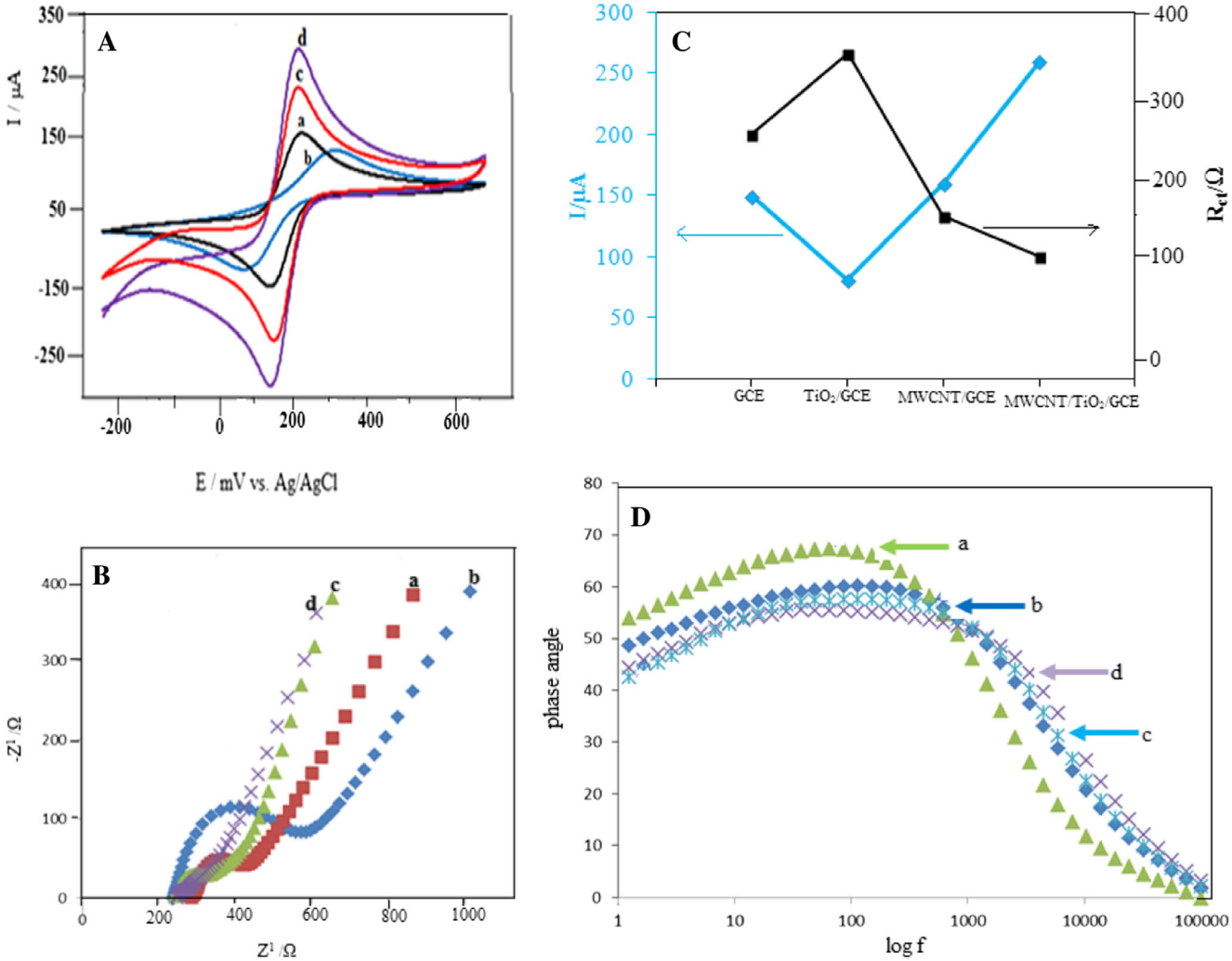

Fig. 3 **a** CVs of the modified GCE in the presence of 1 mM $[Fe(CN)_6]^{3-/4-}$ in 0.1 M KCl at a scan rate of 50 mV s^{-1}. **b** EIS behavior of modified GCE measured by impedance in the presence of 1 mM $[Fe(CN)_6]^{3-/4-}$ in 0.1 M KCl. **c** Plot of i_{pa} and R_{ct} vs. modified GCEs. **d** Bode plots for a: GCE, b: TiO_2, c: MWCNT, and d: TiO_2/MWCNT/GCE

Nitrite detection

Influence of pH

The pH effect on i_{pa} of nitrite (87 μM) at TiO_2/MWCNT/GCE was investigated using CVs in 0.1 M PBS (pH 2–10) at a scan rate of 100 mV s^{-1}. The i_{pa} generated from voltammograms increased from pH 2 to 7 and then decreased to pH 10 (Fig. 4). The i_{pa} below pH 6 is due to the instability of the nitrite in acidic solution and hence its consequent conversion to nitrate [26, 30]. The lack of protons [18, 33] in supporting electrolyte above pH 7 has been suggested as a cause for decrease of i_{pa} and similar trends with different probes have been reported [5, 15, 26, 34, 35]. Consequently, all the subsequent experiments were carried out in PBS at pH 7for the oxidation of nitrite.

Table 1 Summary of electrochemical parameters of modified electrodes

Electrode surface	ΔE_p (mV) $(Fe(CN)_6^{3-/4-}$	R_{ct} (Ω) $(Fe(CN)_6^{3-/4-}$	Background corrected i_{pa} (μA) NO_2^-	ΔE_p (mV) presence of NO_2^-
Bare GCE	92	295	7.8	1100
TiO_2/GCE	102	390	4.9	1080
MWCNT/GCE	85	190	11.0	751
TiO_2/MWCNT/GCE	80	88	18.8	750

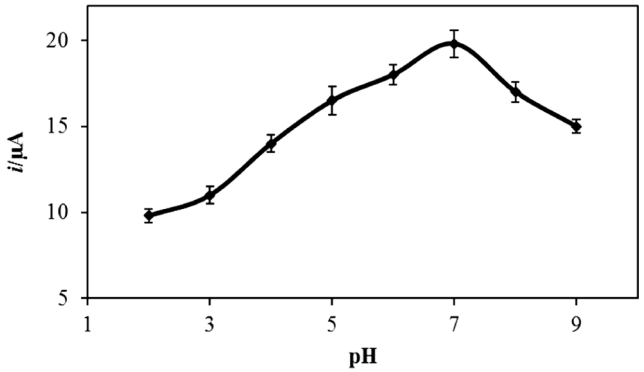

Fig. 4 Effect of solution pH on the i_{pa} of 87 μM NO_2^- at the TiO_2/MWCNT/GCE in 0.1 M PBS

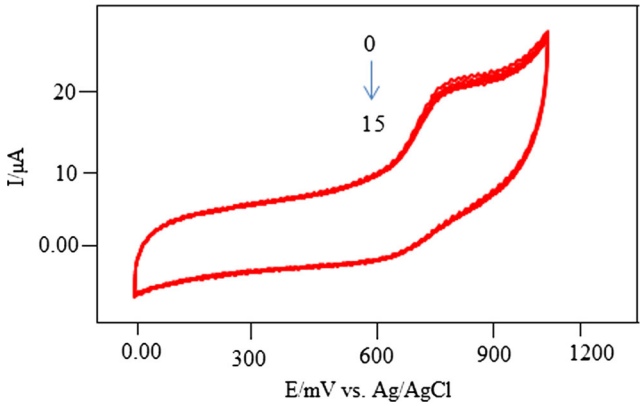

Fig. 6 Continuous cyclic voltammograms for TiO_2/MWCNT/GCE in 87 μM NO_2^- in 0.1 M PBS (pH 7.0) at 100 mV s^{-1}

Cyclic voltammetry detection of nitrite

The voltammogram in 0.1 M PBS (pH 7) showing only background current before addition of nitrite using GCE probe is shown (Fig. 5a). The overpotentials ranging from 750 to 1100 mV for the oxidation of nitrite is shown by the probes prepared. It can be observed that the use of MWCNT in combination with TiO_2 significantly lowered the overpotential, compare the GCE (1100 mV) and TiO_2/GCE (1080 mV) with TiO_2/MWCNT/GCE (750 mV). A negative shift of 250 mV of TiO_2/MWCNT/GCE compared to GCE was deduced. However, the background corrected currents also improved, compare TiO_2/MWCNT/GCE (i_{pa} = 18.8 μA) with GCE (i_{pa} = 7.8 μA), TiO_2/GCE (i_{pa} =

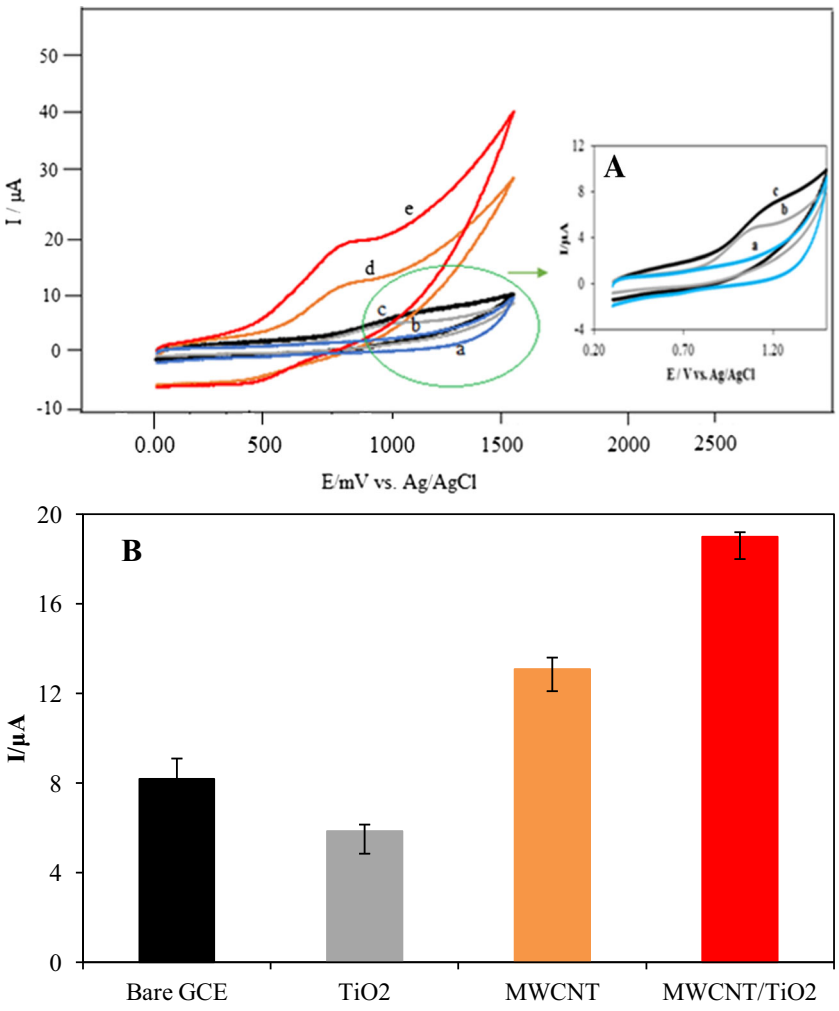

Fig. 5 CVs of GCE in the absence of NO_2^- (a) TiO_2/GCE, (b) GCE, (c) MWNCT/GCE, (d) TiO_2/MWCNT/GCE, and (e) in the presence of 87 μM NO_2^- in 0.1 M PBS (pH 7.0) at 100 mV s^{-1}; error bar = ± S.D. and n = 3. *Inset B*: bar graph of i_{pa} vs. modified electrodes

4.9 μA), and MWCNT/GCE (i_{pa} = 12.0 μA) (Table 1 and Fig. 5a, b *inset*). The enhancement in i_{pa} of TiO_2/MWCNT/GCE is due to good conductivity of nanotubes. The behavior of nitrite on TiO_2/MWCNT/GCE was checked through successive scans (Fig. 6). The electrode was characterized by a very small reduction in i_{pa} showing more stability and suggesting more usability.

Kinetic studies for nitrite detection

The detection of nitrite at different scan rates on the modified electrode was investigated (Fig. 7). E_{pa} shifted to more positive values with increasing scan rate (v) showing that the reaction is irreversible [14]. Further, a linear dependence of i_{pa} on $v^{1/2}$ from 10 to 175 mV s^{-1} (Fig. 7 *inset*) [36] suggests a diffusion-controlled process on the electrode.

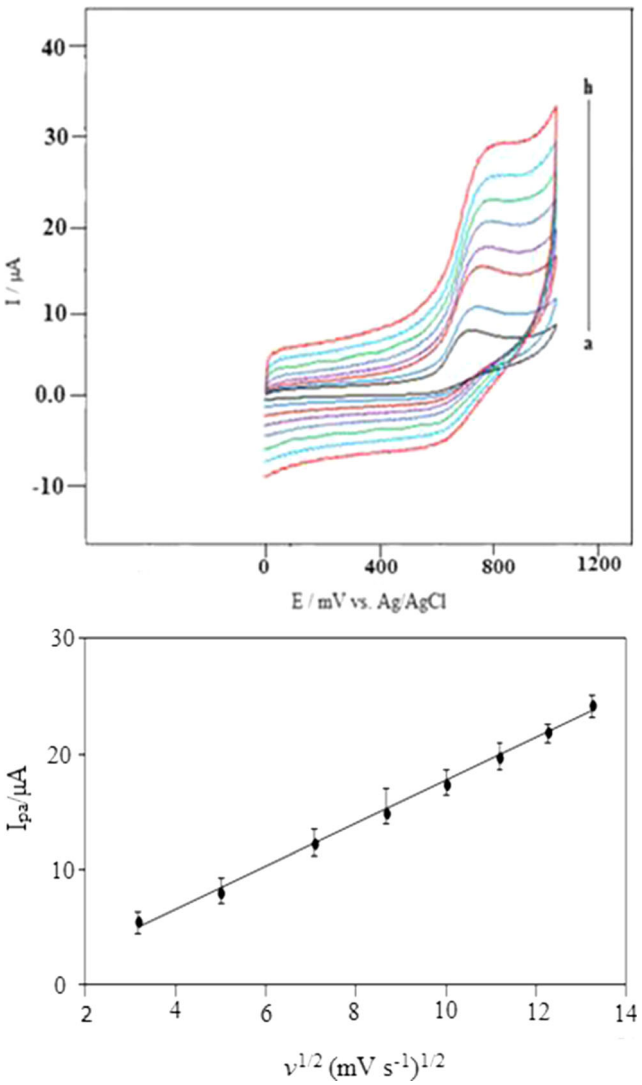

Fig. 7 CVs of TiO_2/MWCNT/GCE in 0.1 M PBS (pH 7.0) containing 87 μM nitrite, (a–h) correspond to 10, 25, 50, 75, 100, 125, 150, and 175 mV s^{-1}. *Inset*: i_{pa} vs. $v^{1/2}$, error bar = ± S.D., and n = 3

The electrons involved in oxidation process were calculated using information form CV. Using E_{pa} = 750 mV, $E_{p/2}$ = 693 mV and substituting into Eq. 1, αn_a = 0.84 which finally gives "n" 1.67 (ca. 2) by assuming electron transfer coefficient (α) of 0.5 [37].

$$E_p - E_{p/2} = 47.7/\alpha n_a \text{ mV at } 25^{\circ}\text{C} \quad (1)$$

Linear sweep voltammetry detection of nitrite was investigated from 1.0 to 18 μM at the modified electrode (Fig. 8). The i_{pa} increased with a slight negative shift in E_{pa} upon each successive addition of nitrite. A plot of i_{pa} vs. [NO_2^-] gave a

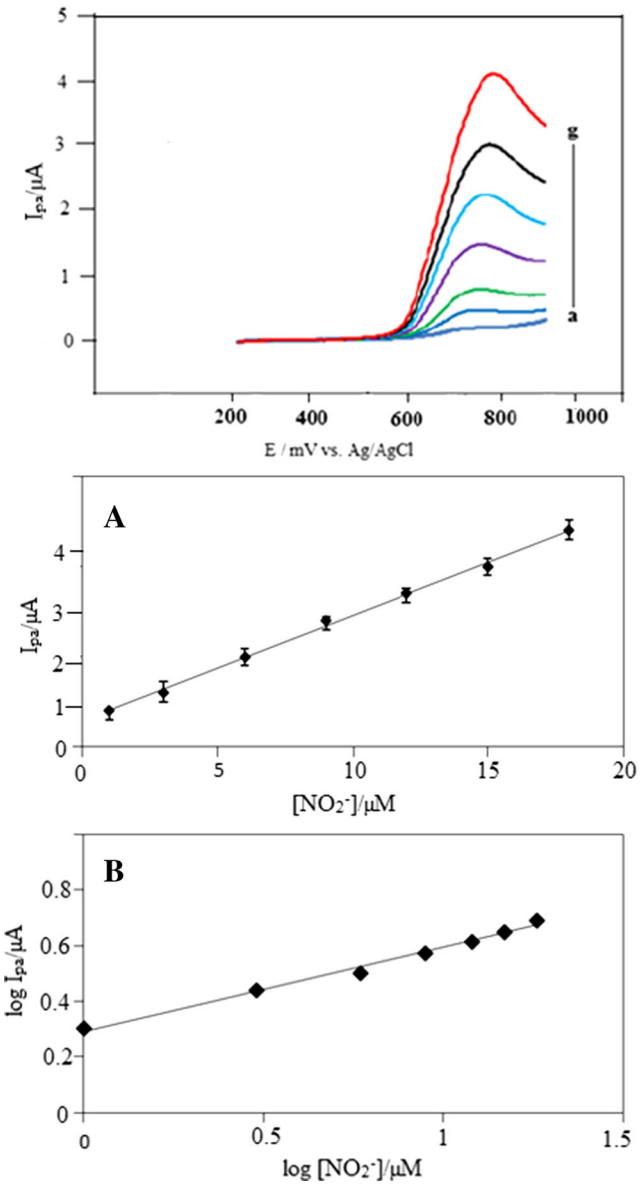

Fig. 8 LSVs obtained for nitrite in the concentrations ranging from 1.0 to 18 μM (a–g), when nitrite was added in steps of 3 μM each in 0.1 M PBS (pH 7). *Inset* **A**, shows calibration plot and **B** shows plot of log i_{pa} vs. log [NO_2^-]; error bar = ± S.D. and n = 3

linear relationship (Fig. 8 *inset* A). Furthermore, the linear relationship from a plot of log i_{pa} vs. log [NO_2^-] (Fig. 8 *inset* B) implies first-order kinetics with respect to the analyte.

Chronoamperometry

The diffusion coefficient (D) was calculated using information from chronoamperometry (Fig. 9). A plot of i vs. $t^{-1/2}$ (Fig. 9a, *inset*) with the best fits for different concentrations of nitrite is shown. Additional, plot of slopes vs. [NO_2^-], is also given (Fig. 9b, *inset*). From the resulting slope and Cottrell equation [36], an average value of D ($= 2.15 \times 10^{-6}$ cm^2 s^{-1}) was deduced and is close to those reported [1, 2].

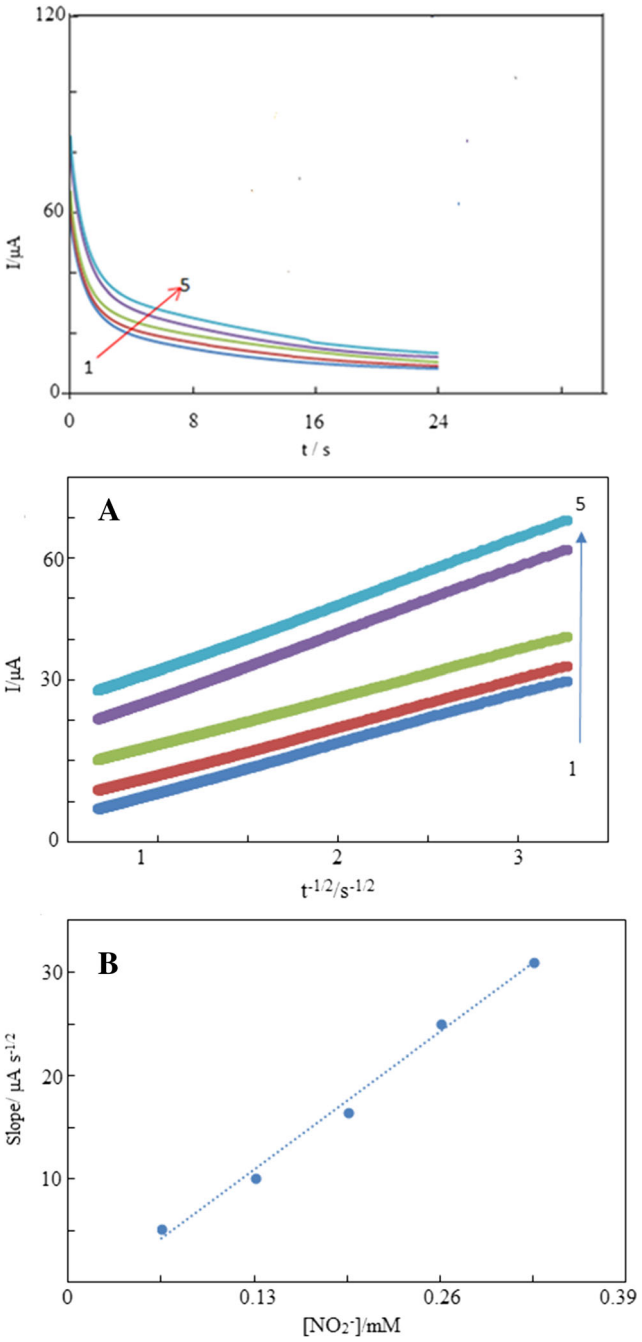

Fig. 9 Chronoamperograms obtained at TiO_2/MWCNT/GCE in 0.1 M PBS (pH 7.0) containing different concentration of NO_2^-. Curves of 1–5 correspond to 0.02, 0.05, 0.15, 0.25, and 0.35 mM NO_2^- for a potential step of 0.95 V. *Inset*: **a** Plots of i vs. $t^{-1/2}$. **b** Slope vs. [NO_2^-]/mM

Differential pulse voltammetry

To demonstrate the ability of TiO_2/MWCNT composite as good sensor candidate for voltammetric traces is one of the important characteristics. In this work, differential pulse voltammograms (Fig. 10) gave a detection limit (LOD) of 0.011 μM calculated using 3 s/b, where s is the standard deviation of the i_{pa} of blank ($n = 10$) and b is the slope of the calibration plot. It can also be seen that current increased linearly with nitrite concentration in the range of 0.02 to 600 μM (Fig. 10, *inset*) and a sensitivity of 0.289 μA μM^{-1} is reported. The results are much improvement to literature values (Table 2) as shown by good stability of composite on the electrode.

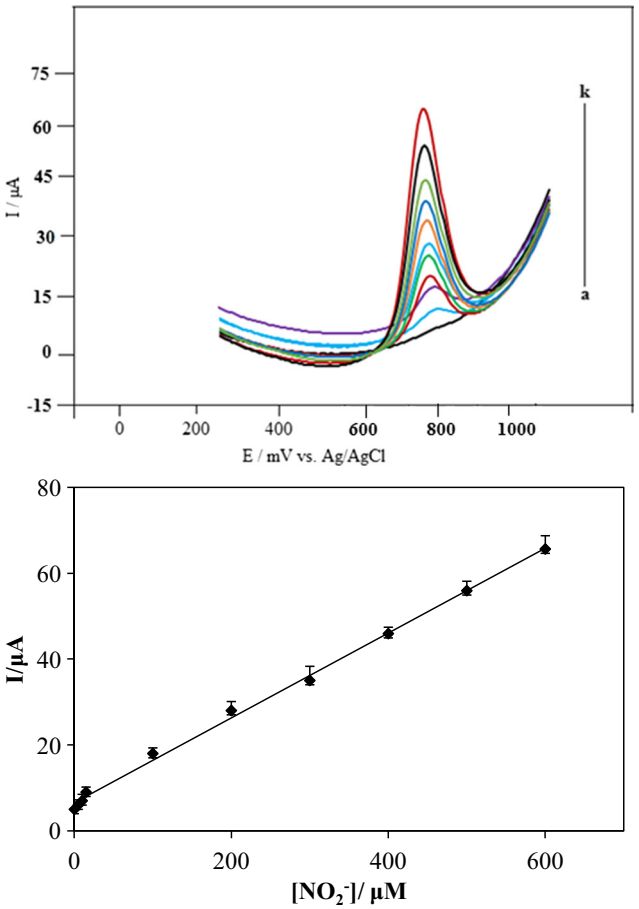

Fig. 10 DPV as a function of different nitrite concentrations (a) blank (PBS pH 7.0), (b) 0.02 μM, (c) 5 μM, (d) 10 μM, (e) 15 μM, (f) 100 μM, (g) 200 μM, (h) 300 μM, (i) 400 μM, (j) 500 μM, and (k) 600 μM. *Inset*: corresponding calibration plot of i_{pa} vs. [NO_2^-, error bar = ± S.D., and $n = 3$

Table 2 Comparison of different chemically modified electrodes for the determination of nitrite with the present fabricated sensor

Modified electrode	Detection technique	Linear range	Detection limit (μM)	Reference
GNPs/MWCPE	SWV	0.05–250.0 μM	0.01	[2]
GO-PANI	Amperometry	0.1–200 μM	0.01	[5]
Zirconium dioxide nanoparticles	Amperometry	0.5–1100	0.3	[15]
Cobalt oxide nanoparticles	Amperometry	0.5–249 μM	0.3	[22]
Fe_2O_3	DPV	0.05–780 μM	0.015	[24]
Ag-PAMAM/GCE	Amperometry	4–1440 μM	0.40	[34]
GCE	Amperometry	2.5–10 μM	0.40	[38]
POA		2.0–5.0	1.05	[39]
Hb/Au-modified electrode		0.4–14.8	0.065	[40]
TiO_2/MWCNT	DPV	0.02 to 600 μM	0.011 μM	Present work

GNPs/MWCPE gold-nanoparticles/multiwalled carbon nanotube/carbon paste, *Ag-PAMAM/GCE-silver* nanoparticles-polyamidoamine, *POA* poly (o-anisidine)

Interference study

Interference measurements were performed using the mixed-solution method (mixing the interferents at different concentrations with 200 μM nitrite in 0.1 M PBS pH 7.0) using differential pulse voltammetry. The peak current change was less than 10% after 100-fold concentration of Mg^{2+}, Ca^{2+}, Zn^{2+}, Cu^{2+}, and Na^{+} and 20-fold concentration of ascorbic acid and urea. It was observed that metal ions have minimal effect on the detection of nitrite at the sensor surface. This was attributed to excellent solubility of the metals nitrites in aqueous media (see Table 3). The obtained results and proposed sensor have a good selectivity during electrochemical analysis.

Analytical applications

The practical applicability of the proposed method using the TiO_2/MWCNT/GCE sensor was investigated by analysis of nitrite in samples from a dam receiving waste from treatment plant. The samples were collected from three different locations in the dam and analyzed without any treatment. The standard addition method was used for determination. A 1.0-mL water sample was added into each of the series of the 10-mL volumetric flasks. Nitrite standard solutions of different concentrations were added to the flask, which were made up to volume with 0.1 M PBS (pH 7.0). An aliquot of 3.0 mL of the solution was placed in a cell for determination and the results are shown in Table 3. The recoveries were in the range of 96.9–98.9%, which confirmed better analysis of nitrite in aqueous solution. For validation, a UV-Vis was used, and relative error values of less than 10% were obtained (Table 4).

Table 3 Effect of interferents

Interferent	$I_{theoretical}$/μA	$I_{observed}$/μA	% current change
[a]Mg^{2+}	27.00	26.81	− 0.7 ± 0.01
[a]Ca^{2+}	27.00	26.98	− 0.07 ± 0.01
[a]Zn^{2+}	27.00	26.05	− 3.52 ± 0.02
[a]Cu^{2+}	27.00	26.16	− 3.11 ± 0.01
[a]Na^{+}	27.00	26.57	− 1.59 ± 0.02
[b]Ascorbic acid	27.00	28.03	+ 3.81 ± 0.01
[b]Urea	27.00	29.53	+ 9.37 ± 0.02

[a] 100-fold concentration

[b] 20-fold concentration

Conclusion

A stable sensor for nitrite was fabricated by drop dry method using TiO_2/ MWCNT composite and showed appreciably low detection limits. Good recoveries were obtained and ranged from 96.9–98.9%. The constructed electrode offers a decrease

Table 4 Results for determination of nitrite in water samples ($n = 3$)

Samples	Added (μM)	Expected (μM)	Found (μM)	Recovery (%)	UV-Vis (μM)	E^a (%)
1	0	–	4.1	98.9 ± 2.1	4.0 ± 0.1	7.9
	5.0	9.2	9.1			
2	0	–	4.5	97.9 ± 1.5	4.3 ± 0.02	4.7
	5.0	9.5	9.3			
3	0	–	4.6	96.9 ± 1.8	4.5 ± 0.01	2.2
	5.00	9.6	9.3			

Relative error (E^a): (TiO_2/MWCNT sensor−UV-Vis method/UV-Vis method) × 100%

on overvoltage of nitrite oxidation. The interference study showed no significant changes in the detection of nitrite. The results obtained demonstrate that the sensor could be used as a management tool for assessing the quality of wastewater.

Acknowledgments The authors would like to acknowledge laboratory facilities from *Midlands State University*, *Gweru*, *Zimbabwe*.

Compliance with ethical standards

Conflict of interest The authors declare that have no conflict of interest.

References

1. Jing L (2009) Electrocatalytic oxidation of nitrite at gold nanoparticle-polypyrrole nanowire modified glassy carbon electrode. Chin J Chem 27(12):2373–2378
2. Afkhami A, Soltani-Felehgari F, Madrakian T, Ghaedi H (2014) Surface decoration of multi-walled carbon nanotubes modified carbon paste electrode with gold nanoparticles for electro-oxidation and sensitive determination of nitrite. Biosens Bioelectron 51: 379–385
3. Pandikumar A, Yusoff N, Huang NM, Lim HN (2014) Electrochemical sensing of nitrite using a glassy carbon electrode modified with reduced functionalized graphene oxide decorated with flower-like zinc oxide. Microchim Acta 182(5–6):1113–1122
4. Kamyabi AM, Aghajanloo F (2008) Electrocatalytic oxidation and determination of nitrite on carbon paste electrode modified with oxovanadium(IV)-4-methyl salophen. J Electroanal Chem 614(1): 157–165
5. Ma X, Miao T, Zhu W, Gao X, Wang C, Zhao C, Ma H (2014) Electrochemical detection of nitrite based on glassy carbon electrode modified with gold–polyaniline–graphene nanocomposites. RSC Adv 4(101):57842–57849. https://doi.org/10.1039/C4RA08543D
6. Carpenter SR, Caraco NF, Correll DL, Howarth RW, Sharpley AN, Smith VH (1998) Nonpoint pollution of surface waters with phosphorus and nitrogen. Ecol Appl 8(3):559–568. https://doi.org/10.1890/1051-0761(1998)008[0559:NPOSWW]2.0.CO;2
7. Pandikumar A, Manonmani S, Ramaraj R (2012) TiO_2–Au nanocomposite materials embedded in polymer matrices and their application in the photocatalytic reduction of nitrite to ammonia. Catal Sci Technol 2(2):345–353. https://doi.org/10.1039/C1CY00298H
8. WHO (World health organisation) (2004) Guidelines for drinking water quality, vol Vol. 1, 3rd edn. World Health Organization, Geneva
9. Ferreira IMPLVO, Silva S (2008) Quantification of residual nitrite and nitrate in ham by reverse-phase high performance liquid chromatography/diode array detector. Talanta 745:1598–1602
10. Abbas MN, Mostafa GA (2010) Anal Chim Acta 410(1):185–192. Determination of traces of nitrite and nitrate in water by solid phase spectrophotometry
11. Ahmed AR, Syed AA (2007) Novel reactions for simple and sensitive spectrophotometric determination of nitrite. Talanta 72(4): 1239–1247
12. Kodamatani H, Yamazaki S, Saito K, Tomiyasu T, Komatsu Y (2009) Selective determination method for measurement of nitrite and nitrate in water samples using high-performance liquid chromatography with post-column photochemical reaction and chemiluminescence detection. J Chromatogr A 1216(15):3163–3167. https://doi.org/10.1016/j.chroma.2009.01.096
13. Bi HL, Zhou WH, Wang YH, Dong SJ (2008) Preparation of nanoparticles of bipyridineruthenium and silicotungstate and application as electrochemiluminescence sensor. Electroanalysis 20(9):996–1001. https://doi.org/10.1002/elan.200704145
14. Moyo M, Lehutso RF, Okonkwo OJ (2015) Improved electrooxidation of triclosan at nano-zinc oxide-multiwalled carbon nanotube modified glassy carbon electrode. Sensors Actuators B 209: 898–905. https://doi.org/10.1016/j.snb.2014.12.059
15. Meng Z, Zheng J, Li Q (2015) A nitrite electrochemical sensor based on electrodeposition of zirconium dioxide nanoparticles on carbon nanotubes modified electrode. J Iran Chem Soc 12(6):1053–1060. https://doi.org/10.1007/s13738-014-0565-9
16. Yu C, Guo J, Gu H (2010) Electrocatalytical oxidation of nitrite and its determination based on Au@ Fe_3O_4 nanoparticles. Electroanalysis 22(9):1005–1011. https://doi.org/10.1002/elan.200900465
17. GR X, Xu G, ML X, Zhang Z, Tian Y, Choi HN, Lee WY (2012) Amperometric determination of nitrite at poly (methylene blue)-modified glassy carbon electrode. Kor Chem Soc 33(2):415–419
18. Zhu N, Xu Q, Li S, Gao H (2009) Electrochemical determination of nitrite based on poly (amidoamine) dendrimer-modified carbon nanotubes for nitrite oxidation. Electrochem Commun 11(12): 2308–2311. https://doi.org/10.1016/j.elecom.2009.10.018
19. Adekunle AS, Mamba BB, Agboola BO, Ozoemena KI (2011) Nitrite electrochemical sensor based on prussian blue/single-walled carbon nanotubes modified pyrolytic graphite electrode. Int J Electrochem Sci 9(2011):1439–1453
20. Li SJ, Zhao GY, Zhang RX, Hou YL, Liu L, Pang H (2013) A sensitive and selective nitrite sensor based on a glassy carbon electrode modified with gold nanoparticles and sulfonated graphene. Microchim Acta 180(9–10):821–827. https://doi.org/10.1007/s00604-013-0999-2
21. Gholivand MB, Jalalvand AR, Goicoechea HC (2014) Computer-assisted electrochemical fabrication of a highly selective and sensitive amperometric nitrite sensor based on surface decoration of electrochemically reduced graphene oxide nanosheets with CoNi bimetallic alloy nanoparticles. Mater Sci Eng C 40:109–120. https://doi.org/10.1016/j.msec.2014.03.044
22. Meng Z, Li B, Zheng J, Sheng Q, Zhang H (2011) Electrodeposition of cobalt oxide nanoparticles on carbon nanotubes, and their electrocatalytic properties for nitrite electrooxidation. Michrochim Acta 175(3-4):251–257. https://doi.org/10.1007/s00604-011-0688-y
23. Muzvidziwa T, Moyo M, Okonkwo OJ, Shumba M, Nharingo T, Upenyu Guyo U (2017) Electrodeposition of zinc oxide nanoparticles on multiwalled carbon nanotube-modified electrode for determination of caffeine in wastewater effluent. Int J Environ Anal Chem 97:1–14
24. Radhakrishnan S, Krishnamoorthy K, Sekar C, Wilson J, Kim SJ (2014) A highly sensitive electrochemical sensor for nitrite detection based on Fe_2O_3 nanoparticles decorated reduced graphene oxide nanosheets. Appl Catal B Environ 148:22–28
25. Iijima S (1991) Helical microtubules of graphitic carbon. Nature 354(6348):56–58. https://doi.org/10.1038/354056a0
26. Jain R, Dhanjai (2011) TiO_2-multi walled carbon nanotubes hybrid film sensor for sensing of antiprotozoal agent satranidazole in solubilzed system. J Electrochem Soc 160(8):H474–H480
27. Fan Y, Liu JH, Lu HT, Zhang Q (2011) Electrochemical behavior and voltammetric determination of paracetamol on Nafion/TiO_2–graphene modified glassy carbon electrode. Colloids Surf B 85(2): 289–292. https://doi.org/10.1016/j.colsurfb.2011.02.041
28. Sun YJ, Huang KJ, Zhao SF, Fan Y, Wu ZW (2011) Direct electrochemistry and electrocatalysis of hemoglobin on chitosan-room temperature ionic liquid-TiO_2-graphene nanocomposite film modified electrode. Bioelectrochemistry 82(2):125–130. https://doi.org/10.1016/j.bioelechem.2011.06.007

29. Kumaravel A, Chandrasekaran M (2011) Biocompatible nano TiO_2/nafion composite modified glassy carbon electrode for the detection of fenitrothion. J Electroanal Chem 650(2):163–170. https://doi.org/10.1016/j.jelechem.2010.10.013
30. Xian H, Wang P, Zhou Y, Lu Q, Wu S, Li Y, Wang L (2010) Electrochemical determination of nitrite via covalent immobilization of a single-walled carbon nanotubes and single stranded deoxyribonucleic acid nanocomposite on a glassy carbon electrode. Microchim Acta 171(1–2):63–69. https://doi.org/10.1007/s00604-010-0404-3
31. Jiang J, Fan W, Du X (2014) Nitrite electrochemical biosensing based on coupled graphene and gold nanoparticles. Biosens Bioelectron 51(2014):343–348. https://doi.org/10.1016/j.bios.2013.08.007
32. He B, Chen W (2016) Voltammetric determination of sulfonamides with a modified glassy carbon electrode using carboxyl multiwalled carbon nanotubes. J Braz Chem Soc 27(12):2216–2225
33. Afkhami A, Madrakian T, Ghaedi H, Khanmohammadi H (2012) Construction of a chemically modified electrode for the selective determination of nitrite and nitrate ions based on a new nanocomposite. Electrochim Acta 66:255–264. https://doi.org/10.1016/j.electacta.2012.01.089
34. Ning D, Zhang H, Zheng J (2014) Electrochemical sensor for sensitive determination of nitrite based on the PAMAM dendrimer-stabilized silver nanoparticles. J Electroanal Chem 717:29–33
35. Brylev O, Sarrazin M, Roué L, Bélanger D (2007) Nitrate and nitrite electrocatalytic reduction on Rh-modified pyrolytic graphite electrodes. Electrochim Acta 52(21):6237–6247. https://doi.org/10.1016/j.electacta.2007.03.072
36. Bard AJ, Faulkner LR (2001) Electrochemical methods, fundamentals and applications, 2nd edn. Wiley, New York
37. Afkhami M, Bahram S, Gholami Z, Zand Z (2005) Micell-mediated extraction for the spectrophotometric determination of nitrite in water and biological samples based on its reaction with *p*-nitroaniline in the presence of diphenylamine. Anal Biochemist 336(2):295–299. https://doi.org/10.1016/j.ab.2004.10.026
38. Kozub BR, Rees NV, Compton RG (2010) Electrochemical determination of nitrite at a bare glassy carbon electrode; why chemically modify electrodes? Sensors Actuators B 143((7):539–546
39. Ojani R, Raoof JB, Zamani S (2013) A novel and simple electrochemical sensor for electrocatalytic reduction of nitrite and oxidation of phenylhydrazine based on poly (o-anisidine) film using ionic liquid carbon paste electrode. Appl Surf Sci 271:98–104. https://doi.org/10.1016/j.apsusc.2013.01.132
40. Yuan B, Xu C, Lin L, Shi Y, Li S, Zhang R, Zhang D (2014) Polyethylenimine-bridged graphene oxide–gold film on glassy carbon electrode and its electrocatalytic activity toward nitrite and hydrogen peroxide. Sensors Actuators B 198:55–61. https://doi.org/10.1016/j.snb.2014.03.014